Monitoring global ocean heat content from space geodetic observations to estimate the Earth energy imbalance

Florence Marti[1], Victor Rousseau[1], Michaël Ablain[1], Robin Fraudeau[1], Benoit Meyssignac[2], Alejandro Blazquez[2]

[1]Magellium, Ramonville Saint Agne, 31520, France
[2]Université de Toulouse, LEGOS (CNES/CNRS/IRD/UT3), 31400 Toulouse, France

Correspondence to: Florence Marti (florence.marti@magellium.fr)

Abstract. This study presents an improved space geodetic approach to estimate the global ocean heat content (GOHC) change and the Earth energy imbalance (EEI) over 1993-2022. The EEI exhibits a positive trend of 0.29 W m-2 decade-1, significant at the 90% confidence level, indicating accelerated ocean warming, in line with independent CERES data. The study highlights the importance of comparing various estimates (eg. in-situ based GOHC) and their uncertainties, to reliably assess EEI changes.

1 Introduction

The ocean absorbs almost all the excess energy stored by the Earth system that results from the anthropogenic greenhouse gas emission in the form of heat (~91%; von Schuckmann et al., 2023; Foster et al., 2021). As the ocean acts as a huge heat reservoir, global ocean heat content (GOHC) is therefore a key component in the Earth's energy budget. An accurate knowledge of the GOHC change allows us to assess the Earth energy imbalance (EEI), which refers to the difference between the amount of energy the Earth receives from the sun and the amount of energy it radiates and reflects back into space. A community effort (Meyssignac et al., 2019) depicted the various methodologies to estimate EEI from the GOHC, including the use of ocean in-situ temperature and salinity profiles (von Schuckmann et al., 2023), the measurement of the ocean thermal expansion from space geodesy (Marti et al., 2022; Hakuba et al., 2021), ocean reanalysis (Stammer et al., 2016), and surface net flux measurements (Kato et al., 2018; L'Ecuyer et al., 2015). Among these approaches, the space geodetic approach, detailed in Marti et al. (2022), leverages the maturity of satellite altimetry and gravimetry measurements to enable precise, extensive spatial and temporal coverage, and full-depth estimates of ocean thermal expansion. As the EEI magnitude is small (0.5-1.0 W m^{-2}, von Schuckmann et al., 2023) compared to the amount of energy entering and leaving the climate system (~340 W m^{-2}, L'Ecuyer et al. 2015), a high level of precision and accuracy are required to estimate the EEI mean (< 0.3 W m^{-2}) and its time variations at decadal scale (< 0.1 W m^{-2}; Meyssignac et al., 2019). In this regard, the space geodetic approach emerges as a promising candidate capable of meeting the stringent EEI precision and accuracy requirements (Meyssignac et al., 2019; Marti et al., 2022).

In this study, our primary objective is to present the updated space geodetic GOHC and EEI estimates and the improvement since Marti et al. (2022), including several major evolutions in the input data, algorithms and a temporal extension into the past, since 1993. The secondary objective is to compare this updated space geodetic monthly GOHC product with GOHC time series derived from in-situ observations. To ensure a consistent and homogeneous treatment, we apply the same processing method to estimate the EEI from the different yearly GOHC time series considered. The obtained EEI estimates are then compared to the net flux at the top of atmosphere (TOA) derived from the Clouds and the Earth's Radiant Energy System (CERES) mission, which serves as a reference for EEI time variations.

2 Data and method

The space geodetic approach consists in deriving the ocean heat content change from the steric sea level change (i.e. the ocean expansion) inferred by satellite observations. We present here an update of the technique for estimating the GOHC change and the EEI, which relies on existing work (Marti et al., 2022) but also benefits from the progress made more recently at regional scales (Rousseau et al., under revision).

In accordance with Rousseau et al. (under revision), the GOHC change is obtained as the sum of regional ocean heat content (OHC) estimated on a 1°x1° grid. However, the uncertainties, their characterisation and their propagation from the input data until the GOHC change and EEI are made at global scale in a similar manner to Marti et al. (2022).

Space geodetic observations are consistent with those used in Marti et al. (2022). The total sea level change is derived from altimetry sea-level gridded products data from the Copernicus Change Climate Change service (C3S) [1]. A correction for TOPEX-A drift is applied (Ablain et al., 2017) as well as a correction for the Jason-3 radiometer drift (Barnoud et al., 2023). The manometric sea level change is estimated from an update of Blazquez et al. (2018) gravimetric solution ensemble (V1.6) [2]. We identified a sub-sample of this ensemble which relies on a single geocenter correction based on Sun et al. (2016) and whose mean is used as our best estimate of the manometric sea level change.

The space geodetic approach builds on the sea level budget to estimate the steric sea level (SSL) change. As we eventually focus on the GOHC change, we neglect the effect of the halosteric sea level change because the impact of salinity changes on SSL is very small at global scale (see Appendix of Lowe and Gregory, 2006). The OHC change is obtained from the ratio of the SSL change and the integrated expansion efficiency of heat (IEEH) coefficient. Knowledge of the warming pattern is a prerequisite to estimate the IEEH. This knowledge relies on in-situ observations. In previous versions, the IEEH was computed from in-situ temperature/salinity profiles (mainly Argo floats) (Rousseau et al., under review). Here the IEEH is computed at regional scale (1°x1°) from temperature/salinity data from the ECCO ocean reanalysis [3]. Using ECCO to estimate the IEEH has an advantage as it allows for the expansion of the spatial area used to compute it. It enables the inclusion of coastal regions up to 100 km from the coastline and deep ocean areas down to 6000 m. We have made the approximation that the IEEH is

constant over time, and equals to its mean value over 2005-2015. This is justified at global scale because the heat pattern of the ocean does not change significantly on decadal time scales (Kuhlbrodt and Gregory, 2012).

In-situ-derived global IEEH ranges from 1.36 10^{-1} m YJ^{-1} for a depth down to 2000 m to 1.57 10^{-1} m YJ^{-1} for a depth down to 6000 m. Using the ECCO ocean reanalysis [3] instead of in-situ data, yields very similar global IEEH values (see Table 1). Over a larger area the ECCO reanalysis indicates an IEEH of 1.50 10^{-1} m YJ^{-1}. The global IEEH uncertainty of 1 10^{-3} m YJ^{-1} ([5%,95%] confidence interval level) is from Marti et al., (2022). It does not account for the IEEH variability due to the spatial domain.

In this study we propose a temporal extension of the space geodetic estimate of GOHC and EEI into the past from January 1993, the start of precise satellite altimetry. As space gravimetry observations are not available before 2002 (GRACE mission was launched in March 2002), the manometric sea level component is extended into the past with the sum of its individual contributions from Greenland, Antarctica, glaciers and from terrestrial water storage. These are derived from the ESA climate change initiative assessment of the sea level budget since 1993 [4].

After calculating the GOHC, the EEI is then obtained from the time derivative of the GOHC - by applying a central finite difference scheme - and accounting for the heat fraction that is entering the ocean (91%) - the remaining 9% of energy being captured by the atmosphere, land and cryosphere (Forster et al., 2021). As described in Marti et al. (2022), the OHC change needs to be filtered out beforehand by applying a Lanczos low-pass filter at 3 years to remove signals related to ocean-atmosphere exchanges which does not correspond to any response to the top of the atmosphere radiation imbalance (Palmer and McNeall, 2014) and must therefore be removed to infer EEI variations. The following equation summarises how the EEI is derived from GOHC:

$$EEI(t) = \frac{dGOHC_{filtered,adjusted}(t)}{dt} \times \frac{1}{\alpha}, with\ \alpha = 0.91\ , \quad (1)$$

In order to assess the GOHC and EEI estimates, the estimation of their uncertainties is a key point. The method (described in Marti et al., 2022) consists in calculating the error variance-covariance matrices of the global mean sea level (GMSL) change data record and of the barystatic sea level data record and then propagating these error variance-covariance matrices to the GOHC and the EEI estimates. The characterisation of uncertainties is similar to that used by Marti et al. (2022). For the GMSL uncertainties, we use an updated altimetry uncertainty budget provided by Guérou et al. (2022), mainly extended over the Jason-3 period (until 2021). For the barystatic sea level uncertainties, we calculate the dispersion of the gravimetry ensemble [2]. This uncertainty is not centred on the barystatic best estimate (see Figure 1). Besides, an uncertainty on the heat fraction entering the ocean is introduced ([89%, 93%]), defined from the different estimates of the literature (e.g. Church et al., 2011; Levitus et al., 2012; Forster et al., 2021; von Schuckmann et al., 2023). The uncertainty associated with the IEEH once propagated is negligible compared with other sources of uncertainty on the mean EEI (<0.1%). From the covariance matrices, we are able to obtain the uncertainty associated with the means, trends or accelerations in GOHC at any time scales, based on an ordinary least squares regression.

The space geodetic GOHC and EEI estimates [5] are then compared to other estimates mostly based on in-situ data. First, we introduce GOHC estimates based on gridded fields of temperature and salinity derived from in-situ measurements, provided by 5 centres: SIO (Scripps Institution of Oceanography) [6], JAMSTEC version 2021 [7], ISAS20 - IFREMER [8], all three relying on Argo network data; EN4 using two sets of corrections (Cheng et al., 2014; Gouretski and Cheng, 2020) [9], and NOAA (National Oceanic and Atmospheric Administration) [10]. We analyse 2 ocean monitoring indicators (OMIs) delivered by CMEMS [11] and also based on in-situ observations, CORA and hereafter "CORA-2011", CORA processed by von Schuckmann and Le Traon (2011). The CORA-2011 dataset is delivered together with an uncertainty envelope whose estimation is described in von Schuckmann and Le Traon (2011). In addition we compare the space geodetic estimate of the GOHC to the recent Global Climate Observing System (GCOS) ensemble estimate [12] composed of 16 time series based on subsurface temperature measurements and representative of the full water column. For the GCOS GOHC ensemble trend we use the uncertainty indicated in von Schuckmann et al. (2023) for the period 2006-2020. Lastly, we introduce an alternative full-depth GOHC estimate derived from the space geodetic approach (Hakuba et al., 2021) [13] (hereafter "JPL"), whose uncertainty is obtained from an ensemble approach.

Apart from GCOS ensemble and the space geodetic estimates, the different GOHC change estimates are extended with a deep ocean warming estimate of +0.068 W m^{-2} from Purkey and Johnson (2010) to encompass the entire water column and account for the deep ocean's substantial thermal influence below 2000 m. In this way, all different GOHC estimates cover the whole water column down to the bottom and are thus comparable with each other.

Both GCOS ensemble and OMIs are made up of yearly time series, while other estimates are available on a monthly basis, which restricts comparisons to interannual time scales. Comparisons are thus led on the basis of annual time series, both for GOHC trend and EEI variability study. The GOHC change estimates are turned into EEI using the same method as described above, with the only difference that annual time series are linearly interpolated on a monthly time scale beforehand.

The CERES Energy Balanced and Filled (EBAF) product [14] is used as a reference for the EEI variability assessment because it is totally independent and it is known to reproduce precisely the EEI variations with uncertainties of the order of a few tenths of W m^{-2}. Its mean value is anchored with an in-situ product (Lyman and Johnson, 2014).

Datasets used for this study are described in Table 2, both for the calculation of GOHC and EEI estimates and for their intercomparison. All uncertainties are reported in the text with a 5 %–95 % confidence level interval.

3 Results

The monthly space geodetic GOHC change from LEGOS-Magellium over January 1993-May 2022 highlights accumulation of heat in the ocean (86% of the total ocean surface excluding the Mediterranean sea). The trend of +0.75 W m^{-2} provides an estimate of the global ocean heat uptake (GOHU) and the uncertainty range for this accumulation rate is [0.61; 1.04] W m^{-2} meaning the GOHU is significantly positive over 1993-2022.

A comparison is made with the annual GOHC change time series from GCOS (Figure 1). The heat content is an extensive variable and GOHC is therefore highly sensitive to spatial coverage. To ensure more consistency in comparison with GCOS, we constrained the LEGOS-Magellium dataset to an ocean surface comparable to GCOS (up to 60° latitude and for areas more than 300m deep). The impact was found to be low with a trend of 0.73 W m^{-2} over 1993-2022. Despite a higher value for the LEGOS-Magellium dataset, the trend results for 1993-2020 are in agreement within their confidence intervals, with the GCOS trend of 0.60 [0.39; 0.82] W m^{-2} and the LEGOS-Magellium trend of 0.71 [0.58, 0.99] W m^{-2}.

When the GOHC trends are calculated over a shorter period (2005-2019) on their respective available ocean surface (Figure 2), the conclusions are similar to those in Figure 1. GOHC trend results from other estimates are also shown. Note that the GCOS ensemble encompasses CORA and CORA-2011 datasets as well as solutions based on the same in-situ temperature and salinity grids that are used and mentioned in section 2. In general, GOHC estimates exclusively based on in-situ measurements are in agreement within their uncertainty ranges. These estimates are constructed using the same atlas of temperature and salinity profiles. Specifically, the data used to calculate the 5 GOHC from gridded fields covers the same ocean surface. Despite this, their trends show some discrepancies that are due to the data processing such as the selection of valid profiles and gridding algorithm. The comparisons confirm that the LEGOS-Magellium dataset shows a stronger trend in GOHC than datasets relying on in-situ measurements, but still agrees within the 90% confidence level. The JPL space geodetic estimate supports these results and increases our confidence in our method.

Temporal variations of the EEI derived from the monthly LEGOS-Magellium space geodetic dataset agree well with the direct EEI measurements provided by CERES but less so with the EEI derived from the GCOS yearly ensemble (Figure 3). Correlated signals are observed, particularly after 2006. These interannual variations are related to the main coupled ocean-atmosphere climate modes modes such as El Niño or the Pacific Decadal Oscillation (Loeb et al. 2018,Meyssignac et al., 2023) or the atmospheric aerosol content resulting from volcanic eruptions and anthropogenic emissions. The 3 EEI solutions show a trend over their respective periods: 0.29 [0.04;0.56] W m^{-2} $decade^{-1}$ for LEGOS-Magellium over 1993-2022; 0.17 W m^{-2} $decade^{-1}$ [-0.25;0.60] for GCOS over 1993-2020; 0.44 [0.34; 0.55] W m^{-2} $decade^{-1}$ for CERES over 2000-2022. Over the common period 2000-2020, the LEGOS-Magellium dataset shows a positive trend of 0.37 W m^{-2} $decade^{-1}$ in agreement with CERES EEI trend of 0.44 W m^{-2} $decade^{-1}$ and both trends are significant at the 90% confidence level. Given the confidence intervals and good agreement between these independent datasets, these results provide confidence in the observed trend in EEI since 2000, indicating a very likely acceleration in global ocean warming over 2000-2020.

The Taylor diagram in Figure 4 indicates the similarity in terms of temporal variability between all OHC-based EEI and the CERES reference. The dataset's proximity to the blue star determines the degree of agreement and how well it matches CERES estimate of the EEI variability. The GCOS and LEGOS-Magellium products exhibit similar time variations, with a correlation of approximately 0.7, which is comparable to the results of Loeb et al. (2021). The JPL EEI has the highest correlation with CERES data (0.9), but too much variability. In-situ-based products have a correlation range of 0.25 to 0.8, indicating different levels of agreement with CERES.

4 Discussions and conclusions

This study proposes an extended estimate of the GOHC change and the EEI from 1993 onwards using the space geodetic approach. We compare this estimate with various estimates based on in-situ measurements, as well as with the CERES EBAF estimate of the EEI.

Apart from the global measurement by CERES, the studied methods do not yet cover the entire ocean. However, the major advantage of the space geodetic approach is the large and homogeneous sampling of the ocean surface since August 2002, and the integration of the whole water column. The space geodetic GOHC shows a significant trend of +0.75 [0.61;1.04] W m^{-2} and EEI trend of 0.29 [0.04;0.56] W m^{-2} $decade^{-1}$ over the period 1993-2022.

Considering the current knowledge of the uncertainties associated with satellite gravimetry and altimetry data, the comparison of our results with other datasets allows us to cross-check the consistency of the different estimates of the ocean warming rate within a [5%-95%] confidence level interval. However, the higher GOHC trends observed with the space geodetic approach (LEGOS-Magellium and JPL datasets) compared to all in-situ datasets could reveal limitations in the observing systems such as the unobserved deep ocean with in-situ data or systematic errors in space geodetic data, which need to be further investigated.

In addition, the comparison of our space geodetic EEI estimate with the direct EEI estimates provided by the CERES EBAF dataset provides complementary assessment information on the variability of EEI. On the one hand we find a good temporal correlation of the EEI derived from space geodetic and CERES EBAF estimates. On the other hand a significant EEI trend has been detected in both CERES and the space geodetic approach suggesting a very likely acceleration of global ocean warming over the last 20 years.

Data availability

Space geodetic GOHC change and EEI dataset (v5.0) is available online at https://doi.org/10.24400/527896/a01-2020.003 (Magellium/LEGOS, 2020) with the complete associated documentation (product user manual and algorithm theoretical basis document).

Acknowledgements

We would like to first thank Audrey Minière, Karina Von Schuckmann and Lorena Moreira Mendez for their contributions to the preparation of this paper and Françoise Mertz for making the data available on the ODATIS portal and AVISO. We also thank two anonymous reviewers for their constructive comments on earlier drafts of this manuscript.

Financial support

This work has been supported by CNES, both for its development and dissemination. Comparison with other datasets was funded by CNRS. ESA initially supported this work in the framework of the MOHeaCAN project (Monitoring Ocean Heat Content and Earth Energy ImbalANce from Space): https://eo4society.esa.int/projects/moheacan/ (last access: 20 December 2023).

Competing interests

The contact author has declared that none of the authors has any competing interests.

References

Ablain, M., Jugier, R., Zawadki, L., Taburet, N., Cazenave, A., and Meyssignac, B.: The TOPEX-A Drift and Impacts on GMSL Time Series, AVISO Website, October 2017, 2017.

Barnoud, A., Picard, B., Meyssignac, B., Marti, F., Ablain, M., and Roca, R.: Reducing the Uncertainty in the Satellite Altimetry Estimates of Global Mean Sea Level Trends Using Highly Stable Water Vapor Climate Data Records, J. Geophys. Res. Oceans, 128, e2022JC019378, https://doi.org/10.1029/2022JC019378, 2023.

Blazquez, A., Meyssignac, B., Lemoine, J., Berthier, E., Ribes, A., and Cazenave, A.: Exploring the uncertainty in GRACE estimates of the mass redistributions at the Earth surface: implications for the global water and sea level budgets, Geophys. J. Int., 215, 415–430, https://doi.org/10.1093/gji/ggy293, 2018.

Cheng, L., Zhu, J., Cowley, R., Boyer, T., and Wijffels, S.: Time, probe type, and temperature variable bias corrections to historical expendable bathythermograph observations, J. Atmospheric Ocean. Technol., 31, 1793–1825, 2014.

Church, J. A., White, N. J., Konikow, L. F., Domingues, C. M., Cogley, J. G., Rignot, E., Gregory, J. M., Broeke, M. R. van den, Monaghan, A. J., and Velicogna, I.: Revisiting the Earth's sea-level and energy budgets from 1961 to 2008, Geophys. Res. Lett., 38, https://doi.org/10.1029/2011GL048794, 2011.

Consortium, E., Fukumori, I., Wang, O., Fenty, I., Forget, G., Heimbach, P., and Ponte, R. M.: Synopsis of the ECCO Central Production Global Ocean and Sea-Ice State Estimate, Version 4 Release 4, Zenodo, https://doi.org/10.5281/zenodo.4533349, 2021.

DOELLING, D. R.: CERES Energy Balanced and Filled (EBAF) TOA and Surface Monthly means data in netCDF Edition 4.2, https://doi.org/10.5067/TERRA-AQUA-NOAA20/CERES/EBAF_L3B004.2, 2023.

ECCO Consortium, Fukumori, I., Wang, O., Fenty, I., Forget, G., Heimbach, P., & Ponte, R. M. (2023). ECCO Central Estimate (Version 4 Release 4). Retrieved from https://www.ecco-group.org/products-ECCO-V4r4.htm, last access: 14 July 2023

Forget, G., Campin, J.-M., Heimbach, P., Hill, C., Ponte, R., and Wunsch, C.: ECCO version 4: An integrated framework for

non-linear inverse modeling and global ocean state estimation, Geosci. Model Dev., 8, 3071–3104, 2015.
Forster, P., Storelvmo, T., Armour, K., Collins, W., Dufresne, J.-L., Frame, D., Lunt, D., Mauritsen, T., Palmer, M., and Watanabe, M.: The Earth's energy budget, climate feedbacks, and climate sensitivity, 2021.
Foster, J., Smallcombe, J. W., Hodder, S., Jay, O., Flouris, A. D., Nybo, L., and Havenith, G.: An advanced empirical model for quantifying the impact of heat and climate change on human physical work capacity, Int. J. Biometeorol., 65, 1215–1229, https://doi.org/10.1007/s00484-021-02105-0, 2021.
Gaillard, F., Reynaud, T., Thierry, V., Kolodziejczyk, N., and Schuckmann, K. von: In Situ–Based Reanalysis of the Global Ocean Temperature and Salinity with ISAS: Variability of the Heat Content and Steric Height, J. Clim., 29, 1305–1323, https://doi.org/10.1175/JCLI-D-15-0028.1, 2016.
Garcia, H. E., Boyer, T. P., Baranova, O. K., Locarnini, R. A., Mishonov, A. V., and Grodsky, A.: World ocean atlas 2018: Product documentation., 2019.
Good, S. A., Martin, M. J., and Rayner, N. A.: EN4: Quality controlled ocean temperature and salinity profiles and monthly objective analyses with uncertainty estimates, J. Geophys. Res. Oceans, 118, 6704–6716, https://doi.org/10.1002/2013JC009067, 2013.
Gouretski, V. and Cheng, L.: Correction for systematic errors in the global dataset of temperature profiles from mechanical bathythermographs, J. Atmospheric Ocean. Technol., 37, 841–855, 2020.
Guérou, A., Meyssignac, B., Prandi, P., Ablain, M., Ribes, A., and Bignalet-Cazalet, F.: Current observed global mean sea level rise and acceleration estimated from satellite altimetry and the associated uncertainty, All Depths/Remote Sensing/All Geographic Regions/Sea level/Oceans and climate, https://doi.org/10.5194/egusphere-2022-330, 2022.
Hakuba, M. Z., Frederikse, T., and Landerer, F. W.: Earth's Energy Imbalance From the Ocean Perspective (2005–2019), Geophys. Res. Lett., 48, e2021GL093624, https://doi.org/10.1029/2021GL093624, 2021.
Horwath, M., Gutknecht, B. D., Cazenave, A., Palanisamy, H. K., Marti, F., Marzeion, B., Paul, F., Le Bris, R., Hogg, A. E., Otosaka, I., Shepherd, A., Döll, P., Cáceres, D., Müller Schmied, H., Johannessen, J. A., Nilsen, J. E. Ø., Raj, R. P., Forsberg, R., Sandberg Sørensen, L., Barletta, V. R., Simonsen, S., Knudsen, P., Andersen, O. B., Ranndal, H., Rose, S. K., Merchant, C. J., Macintosh, C. R., Von Schuckmann, K., Novotny, K., Groh, A., Restano, M., and Benveniste, J.: ESA Sea Level Budget Closure Climate Change Initiative (SLBC_cci): Time series of global mean sea level budget and ocean mass budget elements (1993-2016, at monthly resolution), version 2.2, https://doi.org/10.5285/17C2CE31784048DE93996275EE976FFF, 2021.
Horwath, M., Gutknecht, B. D., Cazenave, A., Palanisamy, H. K., Marti, F., Marzeion, B., Paul, F., Bris, R. L., Hogg, A. E., Otosaka, I., Shepherd, A., Döll, P., Cáceres, D., Schmied, H. M., Johannessen, J. A., Nilsen, J. E. Ø., Raj, R. P., Forsberg, R., Sørensen, L. S., Barletta, V. R., Simonsen, S. B., Knudsen, P., Andersen, O. B., Randall, H., Rose, S. K., Merchant, C. J., Macintosh, C. R., Schuckmann, K. von, Novotny, K., Groh, A., Restano, M., and Benveniste, J.: Global sea-level budget and ocean-mass budget, with focus on advanced data products and uncertainty characterisation, Earth Syst. Sci. Data, 14, 411–447, https://doi.org/10.5194/essd-14-411-2022, 2022.
Hosoda, S., Ohira, T., Sato, K., and Suga, T.: Improved description of global mixed-layer depth using Argo profiling floats, J.

Oceanogr., 66, 773–787, https://doi.org/10.1007/s10872-010-0063-3, 2010.
Kato, S., Rose, F. G., Rutan, D. A., Thorsen, T. J., Loeb, N. G., Doelling, D. R., Huang, X., Smith, W. L., Su, W., and Ham, S.-H.: Surface Irradiances of Edition 4.0 Clouds and the Earth's Radiant Energy System (CERES) Energy Balanced and Filled (EBAF) Data Product, J. Clim., 31, 4501–4527, https://doi.org/10.1175/JCLI-D-17-0523.1, 2018.
Kolodziejczyk, N., Prigent-Mazella, A., and Gaillard, F.: ISAS temperature and salinity gridded fields, https://doi.org/10.17882/52367, 2021.
Kuhlbrodt, T. and Gregory, J. M.: Ocean heat uptake and its consequences for the magnitude of sea level rise and climate change, Geophys. Res. Lett., 39, https://doi.org/10.1029/2012GL052952, 2012.
L'Ecuyer, T. S., Beaudoing, H. K., Rodell, M., Olson, W., Lin, B., Kato, S., Clayson, C. A., Wood, E., Sheffield, J., Adler, R., Huffman, G., Bosilovich, M., Gu, G., Robertson, F., Houser, P. R., Chambers, D., Famiglietti, J. S., Fetzer, E., Liu, W. T., Gao, X., Schlosser, C. A., Clark, E., Lettenmaier, D. P., and Hilburn, K.: The Observed State of the Energy Budget in the Early Twenty-First Century, J. Clim., 28, 8319–8346, https://doi.org/10.1175/JCLI-D-14-00556.1, 2015.
Legeais, J.-F., Meyssignac, B., Faugère, Y., Guerou, A., Ablain, M., Pujol, M.-I., Dufau, C., and Dibarboure, G.: Copernicus Sea Level Space Observations: A Basis for Assessing Mitigation and Developing Adaptation Strategies to Sea Level Rise, Front. Mar. Sci., 8, 2021.
Levitus, S., Antonov, J. I., Boyer, T. P., Locarnini, R. A., Garcia, H. E., and Mishonov, A. V.: Global ocean heat content 1955-2008 in light of recently revealed instrumentation problems: GLOBAL OCEAN HEAT CONTENT, Geophys. Res. Lett., 36, n/a-n/a, https://doi.org/10.1029/2008GL037155, 2009.
Levitus, S., Antonov, J. I., Boyer, T. P., Baranova, O. K., Garcia, H. E., Locarnini, R. A., Mishonov, A. V., Reagan, J. R., Seidov, D., Yarosh, E. S., and Zweng, M. M.: World ocean heat content and thermosteric sea level change (0–2000 m), 1955–2010, Geophys. Res. Lett., 39, https://doi.org/10.1029/2012GL051106, 2012.
Loeb, N. G., Doelling, D. R., Wang, H., Su, W., Nguyen, C., Corbett, J. G., Liang, L., Mitrescu, C., Rose, F. G., and Kato, S.: Clouds and the Earth's Radiant Energy System (CERES) Energy Balanced and Filled (EBAF) Top-of-Atmosphere (TOA) Edition-4.0 Data Product, J. Clim., 31, 895–918, https://doi.org/10.1175/JCLI-D-17-0208.1, 2018.
Lopez, A.: Sea level daily gridded data from satellite observations for the global ocean from 1993 to present, https://doi.org/10.24381/CDS.4C328C78, 2018.
Lowe, J. A. and Gregory, J. M.: Understanding projections of sea level rise in a Hadley Centre coupled climate model, J. Geophys. Res. Oceans, 111, https://doi.org/10.1029/2005JC003421, 2006.
Lyman, J. M. and Johnson, G. C.: Estimating global ocean heat content changes in upper 1800 m since 1950 and the influence of climatology choice, J. Clim., 27, 1945–1957, https://doi.org/10.1175/JCLI-D-12-00752.1, 2014.
Magellium/LEGOS: Climate indicators from space: Ocean heat content and Earth energy imbalance (V1-0), https://doi.org/10.24400/527896/A01-2020.003, 2020.
Marti, F., Blazquez, A., Meyssignac, B., Ablain, M., Barnoud, A., Fraudeau, R., Jugier, R., Chenal, J., Larnicol, G., Pfeffer, J., Restano, M., and Benveniste, J.: Monitoring the ocean heat content change and the Earth energy imbalance from space

altimetry and space gravimetry, Earth Syst. Sci. Data, 14, 229–249, https://doi.org/10.5194/essd-14-229-2022, 2022.

Meyssignac, B., Boyer, T., Zhao, Z., Hakuba, M. Z., Landerer, F. W., Stammer, D., Köhl, A., Kato, S., L'Ecuyer, T., Ablain, M., Abraham, J. P., Blazquez, A., Cazenave, A., Church, J. A., Cowley, R., Cheng, L., Domingues, C. M., Giglio, D., Gouretski, V., Ishii, M., Johnson, G. C., Killick, R. E., Legler, D., Llovel, W., Lyman, J., Palmer, M. D., Piotrowicz, S., Purkey, S. G., Roemmich, D., Roca, R., Savita, A., Schuckmann, K. von, Speich, S., Stephens, G., Wang, G., Wijffels, S. E., and Zilberman, N.: Measuring Global Ocean Heat Content to Estimate the Earth Energy Imbalance, Front. Mar. Sci., 6, https://doi.org/10.3389/fmars.2019.00432, 2019.

Meyssignac, B., Chenal, J., Loeb, N., Guillaume-Castel, R., and Ribes, A.: Time-variations of the climate feedback parameter λ are associated with the Pacific Decadal Oscillation, Commun. Earth Environ., 4, 1–10, https://doi.org/10.1038/s43247-023-00887-2, 2023.

Monier, M., Derval, C., and Fernandez, E.: EU Copernicus Marine Service Product User Manual for the Global Ocean Heat Content (0-2000m) time series and trend from Reanalysis & Multi-Observations Reprocessing, GLOBAL_OMI_OHC_area_averaged_anomalies_0_2000, Issue 4.0, Mercator Ocean International, https://catalogue.marine.copernicus.eu/documents/PUM/CMEMS-OMI-PUM-GLO-OHC.pdf, last access: 14 July 2023, 2021.

Palmer, M. D. and McNeall, D. J.: Internal variability of Earth's energy budget simulated by CMIP5 climate models, Environ. Res. Lett., 9, 034016, https://doi.org/10.1088/1748-9326/9/3/034016, 2014.

Purkey, S. G. and Johnson, G. C.: Warming of Global Abyssal and Deep Southern Ocean Waters between the 1990s and 2000s: Contributions to Global Heat and Sea Level Rise Budgets, J. Clim., 23, 6336–6351, https://doi.org/10.1175/2010JCLI3682.1, 2010.

Roemmich, D. and Gilson, J.: The 2004–2008 mean and annual cycle of temperature, salinity, and steric height in the global ocean from the Argo Program, Prog. Oceanogr., 82, 81–100, https://doi.org/10.1016/j.pocean.2009.03.004, 2009.

Rousseau, V., Fraudeau, R., Hammond, M., Houndegnonto, O. J., Ablain, M., Blazquez, A., Calafat, F. M., Desbruyères, D., Foti, G., Llovel, W., Marti, F., Meyssignac, B., Restano, M., and Benveniste, J.: Monitoring the regional Ocean Heat Content change over the Atlantic Ocean with the space geodetic approach, Earth Syst. Sci. Data, under review.

von Schuckmann, K., Monier, M., and Drevillon, M.: EU Copernicus Marine Service Quality Information Document for the Global Ocean Heat Content (0-2000m) time series and trend from Reanalysis & Multi-Observations Reprocessing, GLOBAL_OMI_OHC_area_averaged_anomalies_0_2000, Issue 1.0, Mercator Ocean International, https://catalogue.marine.copernicus.eu/documents/QUID/CMEMS-OMI-QUID-GLO-OHC.pdf, last access: 14 July 2023, 2021.

von Schuckmann, K. and Le Traon, P.-Y.: How well can we derive Global Ocean Indicators from Argo data?, Ocean Sci., 7, 783–791, https://doi.org/10.5194/os-7-783-2011, 2011.

von Schuckmann, K., Minière, A., Gues, F., Cuesta-Valero, F. J., Kirchengast, G., Adusumilli, S., Straneo, F., Allan, R., Barker, P. M., Beltrami, H., Boyer, T., Cheng, L., Church, J., Desbruyeres, D., Dolman, H., Domingues, C., García-García, A., Giglio, D., Gilson, J., Gorfer, M., Haimberger, L., Hendricks, S., Hosoda, S., Johnson, G. C., Killick, R., King, B. A.,

Kolodziejczyk, N., Korosov, A., Krinner, G., Kuusela, M., Langer, M., Lavergne, T., Li, Y., Lyman, J., Marzeion, B., Mayer, M., MacDougall, A., Lawrence, I., McDougall, T., Monselesan, D. P., Nitzbon, J., Otosaka, I., Peng, J., Purkey, S., Roemmich, D., Sato, K., Sato, K., Savita, A., Schweiger, A., Shepherd, A., Seneviratne, S. I., Simons, L., Slater, D. A., Slater, T., Smith, N., Steiner, A. K., Suga, T., Szekely, T., Thiery, W., Timmermanns, M.-L., Vanderkelen, I., Wijffels, S. E., Wu, T., and Zemp, M.: Heat stored in the Earth system 1960-2020: Where does the energy go?, 2022.

von Schuckmann, K., Minière, A., Gues, F., Cuesta-Valero, F. J., Kirchengast, G., Adusumilli, S., Straneo, F., Ablain, M., Allan, R. P., Barker, P. M., Beltrami, H., Blazquez, A., Boyer, T., Cheng, L., Church, J., Desbruyeres, D., Dolman, H., Domingues, C. M., García-García, A., Giglio, D., Gilson, J. E., Gorfer, M., Haimberger, L., Hakuba, M. Z., Hendricks, S., Hosoda, S., Johnson, G. C., Killick, R., King, B., Kolodziejczyk, N., Korosov, A., Krinner, G., Kuusela, M., Landerer, F. W., Langer, M., Lavergne, T., Lawrence, I., Li, Y., Lyman, J., Marti, F., Marzeion, B., Mayer, M., MacDougall, A. H., McDougall, T., Monselesan, D. P., Nitzbon, J., Otosaka, I., Peng, J., Purkey, S., Roemmich, D., Sato, K., Sato, K., Savita, A., Schweiger, A., Shepherd, A., Seneviratne, S. I., Simons, L., Slater, D. A., Slater, T., Steiner, A. K., Suga, T., Szekely, T., Thiery, W., Timmermans, M.-L., Vanderkelen, I., Wjiffels, S. E., Wu, T., and Zemp, M.: Heat stored in the Earth system 1960–2020: where does the energy go?, Earth Syst. Sci. Data, 15, 1675–1709, https://doi.org/10.5194/essd-15-1675-2023, 2023.

Stammer, D., Balmaseda, M., Heimbach, P., Köhl, A., and Weaver, A.: Ocean Data Assimilation in Support of Climate Applications: Status and Perspectives, Annu. Rev. Mar. Sci., 8, 491–518, https://doi.org/10.1146/annurev-marine-122414-034113, 2016.

Sun, Y., Riva, R., and Ditmar, P.: Optimizing estimates of annual variations and trends in geocenter motion and J2 from a combination of GRACE data and geophysical models, J. Geophys. Res. Solid Earth, 121, 8352–8370, https://doi.org/10.1002/2016JB013073, 2016.

Table 1: Impact of the depth and the geographical extent considered for the global integrated expansion efficiency of heat (IEEH) coefficient derived from ECCO reanalysis and in-situ data (ISAS20 [8] over 0-2000m and EN4.2.2.l09 [15] for the 2000-6000m layer). The term 'GCOS' in this context refers to the domain on which the Global Climate Observing System ensemble [12] described in von Schuckmann et al. (2023) is estimated. The table presents IEEH values estimated over a comparable extent, with the notable difference being the exclusion of the Mediterranean.

Geographical area and depth	Value of the IEEH coefficient at global scale over the 2005-2015 period (unit: m YJ^{-1})	
	In-situ	**ECCO**
Spatial extent comparable to GCOS, 2000m	0.136	0.135
Spatial extent comparable to GCOS, 6000m	0.157	0.156
Spatial extension near coasts - LEGOS-Magellium dataset V5.0, 6000m	Not available	0.150

343 **Table 2: Data used to calculate the space geodetic ocean heat content change and Earth energy imbalance and to perform**
344 **comparisons.**

Product ref No	Product ID & type	Data access	Reference
1	Sea level gridded data from satellite observations for the global ocean from 1993 to present.	EU Copernicus Climate Change Service, (2018)	Dataset : Lopez, 2018 Publication: Legeais et al. (2021)
2	LEGOS gravimetric (GRACE, GRACE-FO) ensemble of manometric sea level solutions.	LEGOS FTP site: http://ftp.legos.obs-mip.fr/pub/soa/gravimetrie/grace_legos/V1.6/	Update of Blazquez et al., (2018)
3	Estimating the Circulation and the Climate of the Ocean - Central Production Version 4 Release 4 (ECCOv4r4)	NASA ECCO-group website	Dataset: Consortium et al., 2023. Publication: Forget et al., 2015; Consortium et al., 2021.
4	Mass contributions to global mean sea level - dataset of the European Space Agency Sea Level Budget Closure Climate Change Initiative (SLBC_cci)	CEDA archive	Dataset: Horwath et al., 2021. Publication: Horwath et al., 2022
5	LEGOS-Magellium GOHC change/EEI dataset, v5.0	CNES AVISO website	Dataset: Magellium/LEGOS, 2020 Documentation: Algorithm Theoretical Basis Document and Product User Manual
6	Scripps institution of oceanography (SIO) - Roemmich-Gilson Argo Climatology	UCSD SIO Argo website: https://sio-argo.ucsd.edu/RG_Climatology.html	Publication: Roemmich and Gilson, 2009
7	JAMSTEC Argo product - Grid Point Value of the Monthly Objective Analysis using the Argo data (MOAA GPV), version 2021	JAMSTEC website : https://www.jamstec.go.jp/argo_research/dataset/moaagpv/moaa_en.html	Publication: Hosoda et al., 2010
8	ISAS20 temperature and salinity gridded fields	SEANOE - Sea Scientific Open Data Publication	Dataset: Kolodziejczyk et al., 2021 Publication: Gaillard et al., 2016

9	Met Office Hadley Centre observations datasets: EN4.2.2. (c14)	MetOffice website: https://www.metoffice.gov.uk/hadobs/en4/download-en4-2-2.html	Publications: Good et al., 2013; Cheng et al., 2014; Gouretski and Cheng, 2020.
10	NOAA (National Oceanic and Atmospheric Administration) - NCEI (National Centers for Environmental Information) product	NCEI-NOAA website : https://www.ncei.noaa.gov/access/global-ocean-heat-content/	Publication: Levitus et al., 2012; Garcia et al., 2019
11	GLOBAL_OMI_OHC_area_averaged_anomalies_0_2000; Numerical models, In-situ observations, Satellite observations	EU Copernicus Marine Service Product, 2021.	Quality Information Document (QUID): von Schuckmann et al., 2021. Product User Manual (PUM): Monier et al., 2021
12	GCOS EHI Experiment 1960-2020	World Data Center for Climate at DKRZ	Dataset: von Schuckmann et al., 2022. Publication: von Schuckmann et al., 2023.
13	JPL GOHC change dataset from space data	https://zenodo.org/records/5104970	Publication: Hakuba et al., 2021
14	CERES Energy Balanced and Filled (EBAF) TOA and Surface Monthly means data in netCDF Edition 4.2.	NASA Atmospheric Science Data Center	Dataset: DOELLING, 2023 Publications: Loeb et al., 2018; Kato et al., 2018.
15	Met Office Hadley Centre observations datasets: EN4.2.2. (l09)	MetOffice website: https://www.metoffice.gov.uk/hadobs/en4/download-en4-2-2.html	Publications: Good et al., 2013; Levitus et al., 2009.

345

Figure 1: Global ocean heat content change over 1993-2022 depicted by the LEGOS-Magellium space geodetic dataset (red curve) and the GCOS dataset available until 2020 (purple curve). The LEGOS-Magellium dataset is characterised by its standard uncertainty envelope (68% confidence level). The ocean surface considered for the LEGOS-Magellium dataset is comparable to that of the GCOS ensemble (von Schuckmann et al., 2023). Trends are estimated at 5-95% confidence interval level and refer to the top-of-atmosphere surface.

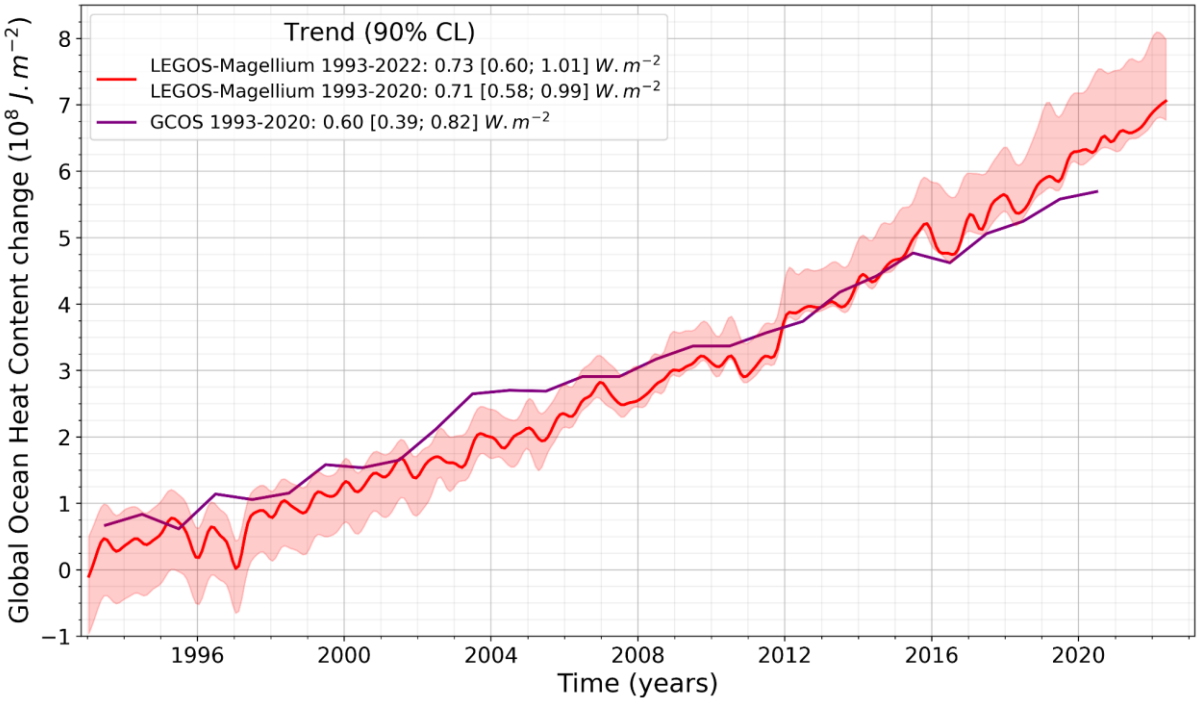

Figure 2: Global ocean heat content (GOHC) trends over the period 2005-2019 from the LEGOS-Magellium (red) and JPL (blue) space geodetic datasets, the GCOS ensemble (purple), in-situ-based GOHC change time series (brown tones), and the 2 CMEMS indicators (green tones). Trends are computed from annual time series and refer to the top-of-atmosphere surface and the indicated trend intervals correspond to the [5-95%] confidence interval level.

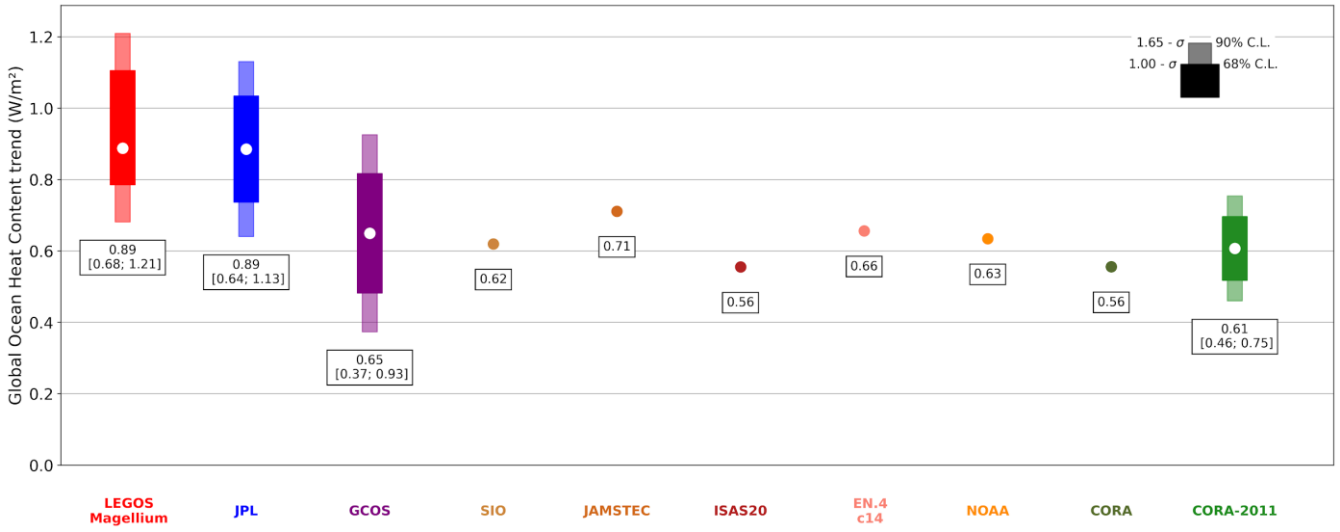

Figure 3: Earth energy imbalance (EEI) time series derived from the LEGOS-Magellium space geodetic approach (red curve), GCOS dataset (purple curve) and from satellite CERES measurements (black curve) over 1993-2022. A 3-year filter is applied to the space geodetic GOHC before derivation into EEI. CERES time series is also filtered at 3 years for comparison. Standard uncertainty envelope (68% confidence level) is shown for the space geodetic dataset in light red. EEI trends are given for each dataset on their common availability period 2000-2020 and refer to the top-of-atmosphere surface. Uncertainties are estimated with a [5%-95%] confidence interval level.

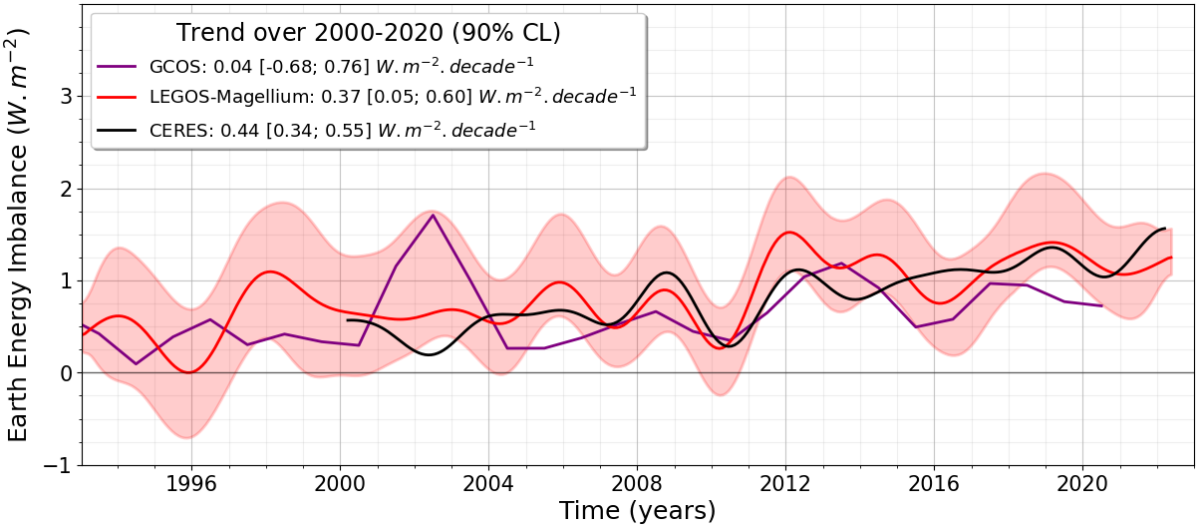

Figure 4: Comparison of Earth energy imbalance (EEI) interannual variations with respect to the CERES dataset (black star) on the 2005-2019 period. Taylor diagram gathering the correlation Pearson coefficient, the centred root means square (W m-2) and the standard deviation (W m-2) for the LEGOS-Magellium (red), JPL (blue), GCOS (purple), in-situ-based EEI (brown tones), and CMEMS indicators (green tones). Results refer to the top-of-atmosphere surface.